بیست و سومین کنفرانس اپتیک و فوتونیک و نهمین کنفرانس مهندسی و فناوری فوتونیک ایران
دانشگاه تربیت مدرس
۱۲-۱۴ بهمن ۱۳۹۵
23rd Iranian Conference on Optics and Photonics and 9th Conference on Photonics Engineering and Technology
Tarbiat Modares University, Tehran, Iran
January 31- February 2, 2017

حسگر ضریب شکست بر مبنای فیلتر شکافی گرافینی

سمیه عسگری و نصرتا... گرانپایه

دانشکده مهندسی برق، دانشگاه صنعتی خواجه نصیرالدین طوسی، تهران، ایران

چکیده – در این مقاله، عملکرد یک حسگر ضریب شکست را با استفاده از روش تحلیلی و نیز روش تفاضل محدود در حوزه‌ی زمان بررسی و شبیه سازی کرده‌ایم. حساسیت حسگر را برای بررسی عملکرد آن محاسبه کرده‌ایم. نتایج تحلیلی و عددی انطباق خوبی با هم دارند. از این ساختار می‌توان در طراحی افزاره‌های نوری در مقیاس نانو و مدارهای مجتمع نوری استفاده کرد.

کلید واژه- پلاسمونیک، تفاضل محدود در حوزه زمان، حسگر ضریب شکست، فیلتر شکافی.

A Refractive Index Sensor Based on the Graphene Notch Filter

Somayyeh Asgari, Nosrat Granpayeh

Faculty of Electrical Engineering, K. N. Toosi University of Technology, Tehran, Iran

Abstract- In this paper, we have analyzed and simulated the performance of a refractive index sensor, by using an analytical and the finite-difference time-domain methods. The sensor sensitivity has been derived to show its sensitivity. The analytical and numerical results comply very well. The proposed device can be utilized in design of the optical nano-scale devices and photonic integrated circuits.

Keywords: Notch filter, Plasmonic, Refractive index sensor.

23rd Conference on Optics and Photonics and 9th Conference on Photonics Engineering and Technology
January 31-February 2 2017

A Refractive Index Sensor Based on the Graphene Notch Filter

S. Asgari

s_asgari@kntu.ac.ir

N. Granpayeh

Granpayeh@kntu.ac.ir

1. Introduction

Graphene, an optical material with one atom thickness has become popular because of its unique optical properties such as low losses, extreme confinement, and tunable conductivity [1-3]. It has been considered as a plasmonic material for constructing nano-scale optical devices and systems for a wide wavelength ranging from near infrared to THz [4].

Recently, different types of graphene plasmonic devices, such as filters [5, 6], sensors [7-9], and switches [10] have been proposed and analyzed theoretically and numerically by using finite-difference time-domain (FDTD) method. Two types of plasmonic modes, the edge and the waveguide modes, are supported by graphene ribbons, which have been analyzed numerically and theoretically. In edge modes, the field is concentrated on the rims of graphene ribbons and can enhance the electromagnetic (EM) coupling to other devices, and in waveguide modes, the field is confined along the entire area of the ribbon [11].

In this paper, by using FDTD numerical method, we have analyzed and simulated the performance of an optical graphene refractive index sensor, composed of two parallel graphene sheets as input and output ports, and a rectangular cavity with the length L. The proposed device will be useful for constructing nano-scale devices in the mid-infrared region for optical processing and computing.

The paper is organized as follows: In Section 2, we have proposed the structure, and refractive index sensitivity. In Section 3 simulation results are given and discussed. The paper is concluded in Section 4.

2. Analytical and Numerical Simulation Methods

2.1. Analytic Approach

The proposed refractive index sensor is depicted in Figure 1. In our simulations, the graphene sheet is assumed as an ultra-thin film with a thickness of Δ in mid-infrared region. The surface conductivity (σ_g) of the graphene layers is governed by the Kubo formula which depends on the momentum relaxation time, τ, temperature, T, chemical potential (Fermi energy), μ_c, and incident angular frequency, ω. At room temperature, the Kubo formula simplifies to [10]:

$$\sigma_g = \frac{ie^2\mu_c}{\pi\hbar^2\left(\omega + i\tau^{-1}\right)} \quad (1)$$

which the intraband transition dominates and the interband transition is neglected [10]. The carrier relaxation time is

$$\tau = -\frac{\mu\mu_c}{ev_f^2} \quad (2)$$

where μ is the carrier mobility and v_f is the Fermi velocity in graphene. The required material parameters of graphene are assumed as: μ=10,000 cm^2/(V.s), v_f=10^6 m/s, and μ_c=0.3 eV. In our simulations, the graphene is treated as an anisotropic dielectric where its in-plane permittivity is [12]:

$$\varepsilon_{eq} = 2.5 + i\,\frac{\sigma_g}{\omega\varepsilon_0\Delta} \quad (3)$$

and the surface-normal dielectric constant component is set as ε=2.5, based on the dielectric constant of graphite. The graphene thickness, Δ, is assumed to be 1 nm [12-14].

Two monitors are put at the points of P_1 and P_2 for measuring the input power, P_{in} and the transmitted power, P_{out}. The transmittance is defined as T=P_{out}/P_{in}. The relationship between wavelengths of transmittance peaks and the cavity length L can be calculated theoretically by the resonance equation of the anti-symmetric coupling resonator [15]:

$$2L = m\lambda \quad (m=1, 2, 3, ...) \quad (4)$$

where λ is the resonance wavelength and m is an integer number. Corresponding to the symmetric

and anti-symmetric magnetic field across the gap between graphene sheets, two SPP modes, symmetric and anti-symmetric, have been appeared [12]. In addition, the wave vector of the anti-symmetric SPP mode supported by double-layer graphene sheets inserted in free space is calculated approximately by [11]:

$$\beta_{AS} \approx k_{spp} + \frac{i\frac{2k_0}{377\sigma_g} - k_p\left(1+u_p\right)}{\frac{\left(1+u_p\right)k_{spp}}{k_p} - u_p k_{spp} h} \qquad (5)$$

where $k_0 = 2\pi/\lambda_0$ is the free space wavenumber, λ_0 is the free space wavelength, $k_{spp} = k_0\left\{1-\left[2/\left(377\sigma_g\right)\right]^2\right\}^{1/2}$ is the wave vector of the SPPs supported by a single-layer graphene, $k_p = \left(k_{spp} - k_0^2\right)^{1/2}$, and $u_p = e^{-k_p h}$. So, the resonance wavelengths can be found by using Eqs. (4) and (5).

2.2. Numerical Approach

In this paper, we have used a two-dimensional FDTD method, with a 12 layer perfectly matched layer absorbing boundary condition around the computation area, and a non uniform mesh in our simulations. The minimum mesh size inside the graphene layer assumed to be 0.1 nm and increases gradually outside the graphene.

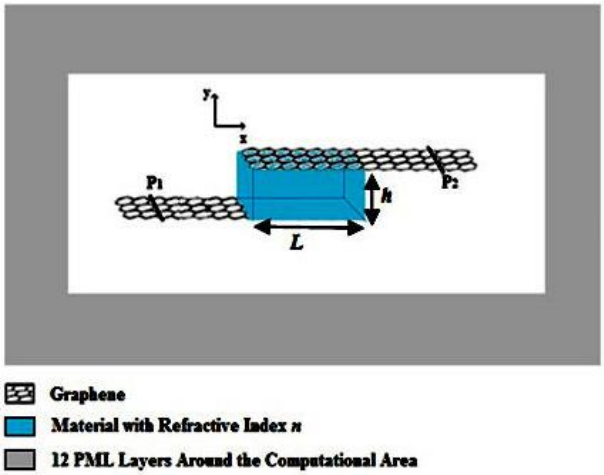

Figure 1: Schematic view of the proposed refractive index sensor with two parallel graphene sheet waveguides and a coupling length *L* between them, *h* is the coupling distance between two graphene sheet waveguides. Two monitors are placed in P_1 and P_2 points for recording the input, and the transmitted power, respectively.

3. Results and Discussion

The resonator was filled with dielectric materials with various refractive indices, *n*, for derivation of refractive index sensitivity. The transmittance spectra with *n*=1, 1.03, 1.06, and 1.09 for *L*= 250 nm, and *h*=50 nm are plotted in Figure 2. By solving Eqs. (4) and (5), the resonance wavelengths of the resonator, according to the second resonance mode of the resonator are derived and plotted in Figure 3.

Transmittance peaks show a red shift with increasing *n*. The value $S=\Delta\lambda/\Delta n$ determines the refractive index sensitivity of the resonance peak. The proposed structure shows a high value of 3300 nm per refractive index unit (nm/RIU) sensitivity to the variations of the refractive indices.

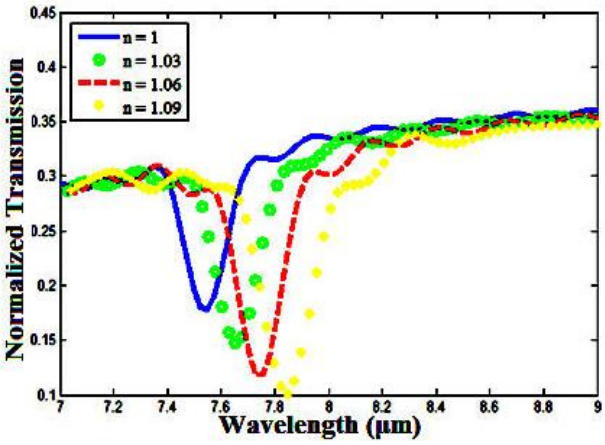

Figure 2: Normalized transmission spectra for four different values of *n* with *L*=250 nm and *h*=50 nm.

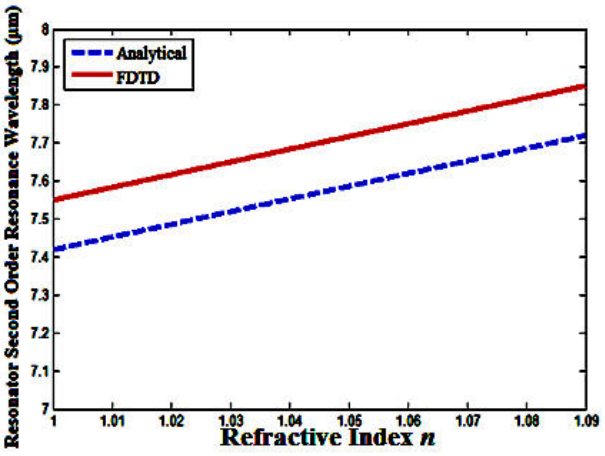

Figure 3: Variations of the second order resonance wavelength of the transmittance versus refractive index, *n* of the material inside the resonator, obtained by the numerical method of FDTD and analytical resonance equation of the resonator, respectively.

In Figure 4, the resonance wavelengths of the sensor as a function of the resonator material

refractive index for different lengths of the resonator are shown. A comparison depicts that the transmittance peaks tend to exhibit a red shift as the resonator length increases.

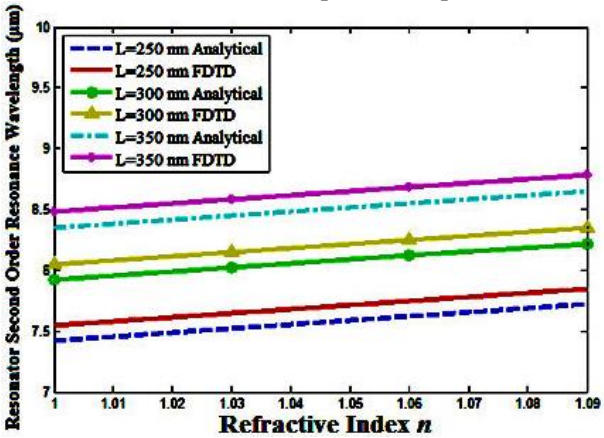

Figure 4: The second order resonance wavelengths of the resonator versus the resonator material refractive index for various resonator lengths.

4. Conclusion

In this paper, two parallel graphene sheets with a coupling length of *L* as a plasmonic sensor is proposed and analyzed analytically and numerically by using the finite-difference time-domain method. A resonance dip occurs in the transmittance pectrum. The sensor shows high refractive index sensitivity. Our study has important applications in integrated plasmonic circuits for sensors.

References

[1] A. K. Geim and S. K. Novoselov, "The rise of graphene," *Nat. Mater*. Vol. 6, No. 3, pp. 183-191, 2007.

[2] F. Bonaccorso, Z. Sun, T. Hasan, and A. C. Ferrari, "Graphene photonics and optoelectronics," Nat. Photonics, Vol. 4, No. 9, pp. 611-622, 2010.

[3] K. S. Novoselov, A. K. Geim, S. V. Morozov, D. Jiang, Y. Zhang, S. V. Dubonos, and A. A. Firsov, "Electric field effect in atomically thin carbon films," *Science*, Vol. 306, No. 5696, pp. 666-669, 2004.

[4] M. Jablan, H. Buljan, and M. Soljacic, "Plasmonics in graphene at infrared frequencies," *Phys. Rev. B*, Vol. 80, No. 24, pp. 1-7, 2009.

[5] M. Danaeifar, N. Granpayeh, A. Mohammadi, and A. Setayesh, "Graphene-based tunable terahertz and infrared band-pass filter," *Appl. Opt.* Vol. 52, No. 22, pp. 68-72, 2013.

[6] H. Nasari and M. S. Abrishamian, "All-optical tunable notch filter by use of Kerr nonlinearity in the graphene microribbon array," *J. Opt. Soc. Am. B*, Vol. 31, No. 7, pp. 1691-1697, 2014.

[7] S-B. Yan, L. Luo, C-Y. Xue, and Zhi-Dong Zhang, "A Refractive Index Sensor Based on a Metal-Insulator-Metal Waveguide-Coupled Ring Resonator," *Sensors*, Vol. 15, No. 11, pp. 29183-29191, 2015.

[8] K. Maharana, T. Srivastava, and R. Jha, "Low index dielectric mediated surface plasmon resonance sensor based on graphene for near infrared measurements," *IEEE. Photon. Technol. Lett*. vol. 47, no. 38, pp. 385102 (1-12), 2014.

[9] A. Dolatabady, N. Granpayeh, and V. Foroughi Nezhad, "A nanoscale refractive index sensor in two dimensional plasmonic waveguide with nanodisk resonator," *Opt. Commun.* Vol. 300pp. 265-268, 2013.

[10] H-J. Li, L. L. Wang, Z. Huang, B. Sun, X. Zhai, and X. Li, "Mid-infrared, plasmonic switches and directional couplers induced by graphene sheets coupling system," *Europhys. Lett.* Vol. 104, No. 3, pp. 3701 (1-5), 2013.

[11] J-P. Liu, X. Zhai, L-L. Wang, H-J. Li, F. Xie, Q. Lin, and S-X. Xia "Analysis of mid-infrared surface plasmon modes in a graphene-based cylindrical hybrid waveguide," *Plasmonics*, Vol. 11, No. 3, pp. 703-711, 2016.

[12] C. H. Gan, H. S. Chu, and E. P. Li, "Synthesis of highly confined surface plasmon modes with doped graphene sheets in the midinfrared and terahertz frequencies," *Phys. Rev. B*, Vol. 85, No. 12, pp. 125431 (1-9), 2012.

[13] W. Gao, J. Shu, C. Qiu, and Q. F. Xu, "Excitation of plasmonic waves in graphene by guided-mode resonances," *ACS. Nano.* Vol. 6, No. 9, pp. 7806–7813, 2012.

[14] A. Vakil and N. Engheta, "Transformation optics using graphene," *Science*, Vol. 332, No. 6035, pp. 1291-1294, 2011.

[15] H-J. Li, L. L. Wang, Z-R. Huang, B. Sun, and X. Zhai "Tunable mid-infrared plasmonic anti-symmetric coupling resonator based on the parallel interlaced graphene pair," *Plasmonics*, Vol. 10, No. 1, pp. 39-44, 2015.